The Astrophysical Journal, 674:511–519, 2008 February 10
© 2008. The American Astronomical Society. All rights reserved. Printed in U.S.A.

A FISK-PARKER HYBRID HELIOSPHERIC MAGNETIC FIELD WITH A SOLAR-CYCLE DEPENDENCE

R. A. Burger, T. P. J. Krüger, M. Hitge, and N. E. Engelbrecht
Unit for Space Physics, Potchefstroom Campus of the North-West University, Potchefstroom, 2520, South Africa; adri.burger@nwu.ac.za
Received 2007 September 18; accepted 2007 October 29

ABSTRACT

We present a refinement of the Fisk-Parker hybrid field of Burger and Hitge which now includes a region bordering the solar rotational equator where magnetic field footpoint motion occurs only through diffusive reconnection. The hybrid field, therefore, only occurs above a certain latitude in a given hemisphere, and in the equatorial region the field is a pure Parker field. We also propose a simple qualitative model for the solar cycle dependence of the hybrid field, taking into account changes in the tilt angle of the heliospheric current sheet and the latitudinal extend of the polar coronal hole on the photosphere and on the source surface over the course of a solar activity cycle. We find that the amplitude of magnetic field fluctuations for assumed solar minimum parameters would not be observable above the background noise (see Roberts and coworkers). We also show that for these parameters, periodicities associated with differential footpoint motion would be barely distinguishable from rigid rotation at the solar equatorial rate. We point out that the question of periodicities in magnetic field data is perhaps more complicated than previously thought. We confirm the result of Burger and Hitge that a Fisk-type heliospheric magnetic field provides a natural explanation for the observed linear relationship between the amplitude of the recurrent cosmic-ray variations and the global latitude gradient (see Zhang). We show that this relationship holds for helium, protons, and electrons. Moreover, we show that the constant of proportionality is larger when $qA > 0$ than when $qA < 0$, as inferred from observations by Richardson and coworkers.

Subject headings: cosmic rays — diffusion — Sun: magnetic fields — turbulence

1. INTRODUCTION

Fisk's model of the heliospheric magnetic field (Fisk 1996) forms the basis of the hybrid field approach of Burger & Hitge (2004). In a Fisk-type field, magnetic field lines exhibit extensive excursions in heliographic latitude, and has been cited as a possible explanation for recurrent energetic particle events observed by the *Ulysses* spacecraft at high latitudes (see, e.g., Simpson et al. 1995; Zhang 1997; Paizis et al. 1999), as well as the smaller than expected cosmic-ray intensities observed at high latitudes (Simpson et al. 1996). Since the original paper by Fisk (1996), the Fisk field and the physics behind it have been discussed in a series of papers by Fisk and his coworkers (see, e.g., Fisk & Schwadron 2001; Fisk 2001, 2005; Fisk & Zurbuchen 2006, and references therein). Fisk assumed that the polar coronal hole is symmetric with respect to the solar magnetic axis, and that the magnetic field expands nonradially to yield a uniform field farther away from the Sun. The footpoints of the magnetic field lines anchored in the photosphere experience differential rotation. Then, if the magnetic axis of the Sun is assumed to rotate rigidly at the equatorial rate, differential rotation will cause a footpoint to move in heliomagnetic latitude and longitude, thus experiencing different degrees of nonradial expansion. The end result is a field line that moves in heliographic latitude, and the simple concept of "field lines on cones" of the Parker field (Parker 1958) breaks down. Over the last 10 years, various attempts to incorporate the Fisk field into numerical modulation models have been reported (Kóta & Jokipii 1997, 1999, 2001; Burger et al. 2001; Burger & Hitge 2002, 2004; Burger & de Jager 2003; Krüger 2005). A recent overview of various models for the heliospheric magnetic field, including Fisk-type fields, is given by Burger (2005).

A key question is of course whether a Fisk-type field actually exists. The analysis of *Ulysses* magnetic field data by Zurbuchen et al. (1997) suggests very strongly that it does. Roberts & Goldstein (1998) report that solar wind seen within about 30° of the magnetic equator actually originates from polar regions, at latitudes larger than about 60° (see, however, Woo et al. 1999), with clear indications of differential photospheric rotation and rigid coronal hole rotation. They find that signatures of the latter two phenomena are also present in magnetic field data. Forsyth et al. (2002) analyzed data from the *Ulysses* spacecraft and do not rule out the existence of a Fisk-type field, but the authors conclude that systematic deviations that would be its signature may have amplitudes too low to be reliably detected in heliospheric magnetic field data from spacecraft such as *Ulysses*. Lionello et al. (2006) use a time-dependent three-dimensional MHD simulation and find that the basic idea of Fisk (1996) that open magnetic field lines do undergo latitudinal excursion is confirmed by their calculations. However, they state that the latitudinal excursion is too small to explain *Ulysses* observations of energetic particles at high latitudes if their transport occurs via direct magnetic connection. They also point out that coronal holes in their models do not rotate strictly rigidly as assumed by Fisk. A recent in-depth analysis of *Ulysses* magnetic field data by Roberts et al. (2007) shows no evidence of a Fisk-type field. Their conclusion is based on predicted field variations for parameters used by Zurbuchen et al. (1997) and they point out that some of these parameters may have been overestimated. They still find the physics of the Fisk field plausible.

No unambiguous conclusion regarding the existence of the Fisk field can be drawn from the above references. We will use results from the detailed analysis of Roberts et al. (2007) to determine whether the Fisk-Parker hybrid field should be observable for the parameters that we use for solar minimum conditions. We will also point out an intriguing consequence of their analysis. Preliminary results for the current project is given by Krüger (2005).

2. THE FISK-PARKER HYBRID FIELD: A SOLAR-CYCLE DEPENDENT APPROACH

The hybrid field approach was first described by Burger & Hitge (2004). They assume that ordered magnetic field footpoint

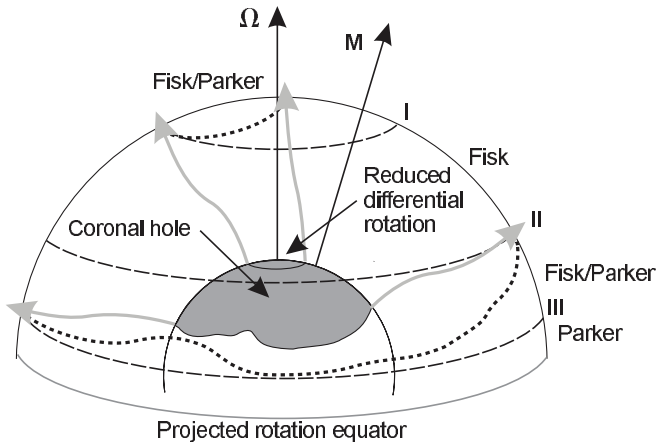


FIG. 1.—Schematic representation of field lines, shown as gray lines with arrowheads, mapping from the photosphere (*inner circle*) to the source surface (*outer circle*). The dotted line on the source surface near the pole represents the region to which an area of reduced or no differential rotation on the photosphere will map to. The lower dotted line on the source surface denotes the actual boundary of the edge of the polar coronal hole, mapped from the photosphere. The magnetic axis is denoted by **M** and the rotation axis by Ω. Not to scale. See text for discussion.

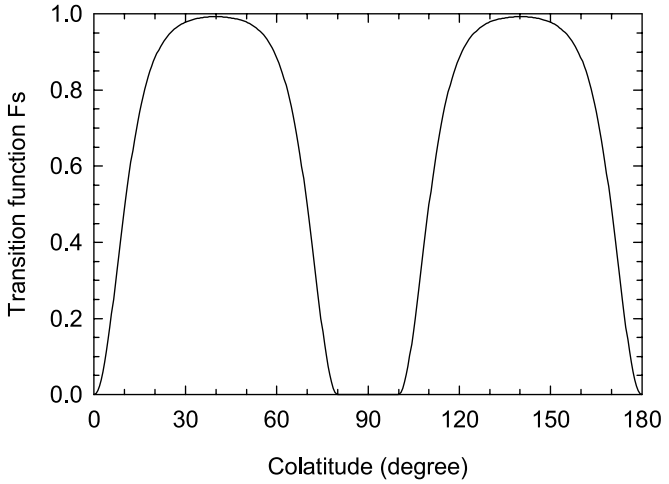


FIG. 2.—Transition function that is used to model the physical situation illustrated in Fig. 1 as function of colatitude. Here it is assumed that the influence of the Fisk field extends to a colatitude of 80°.

motions on the source surface, where the field is essentially radial, persist up to the solar rotational equator. The resulting heliospheric field is therefore a Fisk-Parker hybrid at essentially all latitudes. In the current model we assume that there is a range of latitudes around the solar rotation equator where only diffusive reconnection of magnetic field lines occur, and that ordered footpoint motion only occurs at higher latitudes. The latter region is determined by the mapping of open field lines, originating in an idealized polar coronal hole on the photosphere, to the source surface.

A fully realistic model to map what is happening on the photosphere to the source surface is beyond the scope of this study. Given the complexity of the actual polar coronal holes, especially when the solar magnetic field changes polarity (see, e.g., Fox et al. 1998), this is a daunting task.

The motivation for the current model is shown schematically in Figure 1. We assume that the polar coronal hole is centered on the rotation axis on the photosphere. The mapped region on the source surface will, however, not be centered on this axis on the source surface due to superradial expansion of the magnetic field. The minimum latitude at which ordered footpoint motion can occur is denoted by a dashed line in Figure 1 and labeled III. Between this latitude and the one labeled II in the figure, one would expect a mixture of a region where footpoint motion occurs by means of diffusive reconnection, and another by means of ordered motion. The former leads to a Parker-type field, and the latter to a Fisk-type field (Kobylinski 2001). At lower latitudes than the one labeled III, the field will be Parker-like. Note that the magnetic equator is then always confined between latitude III and its counterpart in the southern hemisphere. Turning now to the highest latitudes, the question is whether differential rotation also occurs in these regions (see, e.g., Schou et al. 1998). For the purpose of the present study we assume that it does not. Given the way one would expect the region denoted by a solid line on the photosphere to map to the source surface, above a certain latitude there should be a region where footpoint motion occurs mainly by means of diffusive reconnection, and another mainly by means of ordered motion. This latitude is denoted by I in Figure 1. We therefore expect that the heliospheric magnetic field that originates from the pole to latitude I the field is a mixture of Parker-type and Fisk-type fields; a pure Fisk-type field from I to II, a mixture of Parker-type and Fisk-type fields from II to III, and a Parker-type between III and the solar rotation equator.

To model this complicated azimuthally dependent situation in a simple way, taking into account the various latitude regions in Figure 1, we use a transition function

$$F_S = \begin{cases} \left\{\tanh\left[\delta_p\theta\right] + \tanh\left[\delta_p(\theta-\pi)\right] \right. \\ \left. -\tanh\left[\delta_e\left(\theta-\theta_b'\right)\right]\right\}^2 & \text{if } 0 \leqslant \theta < \theta_b', \\ 0 & \text{if } \theta_b' \leqslant \theta \leqslant \pi - \theta_b', \\ \left\{\tanh\left[\delta_p\theta\right] + \tanh\left[\delta_p(\theta-\pi)\right] \right. \\ \left. -\tanh\left[\delta_e(\theta-\pi+\theta_b')\right]\right\}^2 & \text{if } \pi-\theta_b' < \theta \leqslant \pi, \end{cases} \quad (1)$$

which is illustrated in Figure 2 and is similar to the one used by Burger & Hitge (2004). The parameters δ_p and δ_e are used to control the transition from predominantly Fisk-type to Parker-type fields at the poles and equator, respectively. The parameter θ_b' corresponds to the latitude III in Figure 1.

The velocity field of Burger & Hitge (2004) must be modified in order to reflect the refinements discussed above. The new divergence-free velocity field for the refined Fisk-Parker hybrid magnetic field in the frame corotating with the Sun is given by

$$\begin{aligned} u_\theta &= r_0\omega^* \sin\beta^* \sin\phi_\Omega, \\ u_\phi &= r_0\Big(\omega^* \sin\beta^* \cos\theta\cos\phi_\Omega + \omega^* \cos\beta^* \sin\theta \\ &\quad + \frac{d\omega^*}{d\theta} \sin\beta^* \sin\theta\cos\phi_\Omega \\ &\quad + \omega^* \frac{d\beta^*}{d\theta} \cos\beta^* \sin\theta\cos\phi_\Omega\Big), \end{aligned} \quad (2)$$

with

$$\begin{aligned} \beta^*(\theta) &= \beta F_S(\theta), \\ \omega^*(\theta) &= \omega F_S(\theta), \end{aligned} \quad (3)$$

where F_S is the transition function (eq. [1]) and β and ω have constant values. Here θ and ϕ_Ω are heliographic colatitude and

azimuth, respectively, r_0 is the radius of the source surface, and ω is the differential rotation rate. To define the angle β, note that a field line originating at the heliographic pole suffers no differential rotation and therefore always maps to the same point on the source surface, from where it is transported radially outward by the solar wind, thus defining a virtual axis, denoted by p in Figure 3. The angle between this axis and the rotation axis of the Sun, denoted by Ω, is β.

In order for the velocity field (eq. [2]) to be divergence-free, the only constraint on F_S is that it must only depend on θ. This will ensure that the heliospheric magnetic field derived from it (see, e.g., Giacalone 1999) is also divergence-free.

Figure 3 shows the trajectories of magnetic field footpoints on the source surface. We used values $\alpha = 12^\circ$ (see below for relation to β), $\omega = \Omega/4$, $\delta_p = 5.0$, and $\delta_e = 5.0$ to produce Figure 3, the same as in the numerical modulation code discussed in § 4. Random motion of magnetic field footpoints is not shown but will be superimposed on these trajectories and will be the only kind of footpoint motion that occurs in the shaded region bordering the solar rotation equator in this figure. The effect of random footpoint motion on the heliospheric magnetic field is discussed by Giacalone (1999, 2001). If one considers direct numerical simulation of particle transport (see, e.g., Giacalone 2001; Pei et al. 2006) the effect of these random motions of the background field should be taken into account directly. Giacalone et al. (2006) show that a two-component model of interplanetary turbulence can be generated from a quasi-static model with a suitable choice of spacetime variations of the footpoint motions of magnetic fields on a source surface. Since we will use a two-component slab/two-dimensional model for turbulence in our diffusion tensor, random footpoint motion is incorporated indirectly in our modulation model.

For the purpose of the present study it is assumed that the Parker field is unaffected by differential rotation. Therefore, both the angle β and the differential rotation rate ω must become zero where the field is Parker-like, or equivalently, in the hybrid field model they must scale with F_S. These parameters are therefore multiplied by F_S to give the effective latitude-dependent functions.

The Fisk-Parker hybrid heliospheric magnetic field in the fixed observer's frame that follows from the velocity field (eq. [2]) is given by

$$
\begin{aligned}
B_r &= A\left(\frac{r_0}{r}\right)^2, \\
B_\theta &= B_r \frac{r}{V_{\rm sw}} \omega^* \sin\beta^* \sin\phi^*, \\
B_\phi &= B_r \frac{r}{V_{\rm sw}} \left[\omega^* \sin\beta^* \cos\theta \cos\phi^* \right. \\
&\quad + \sin\theta(\omega^* \cos\beta^* - \Omega) + \frac{d\omega^*}{d\theta} \sin\beta^* \sin\theta \cos\phi^* \\
&\quad \left. + \omega^* \frac{d\beta^*}{d\theta} \cos\beta^* \sin\theta \cos\phi^* \right], \qquad (4)
\end{aligned}
$$

where $\phi^* = \phi - \Omega t + \Omega(r - r_0)/V_{\rm sw} + \phi_0$, A is a signed constant [magnitude $|B_r(r_0)|$; positive when the field in the northern hemisphere is directed away from the Sun, and negative when it's directed toward the Sun], and $V_{\rm sw}$ is the (constant and radial) solar wind speed. The other quantities are defined in equation (2).

These equations are easily extended for the case when the solar wind speed depends on latitude (Schwadron 2002). When $F_S = 1$ the equations reduce to those presented by Zurbuchen et al. (1997) and when $F_S = 0$, the standard Parker field (Parker 1958).

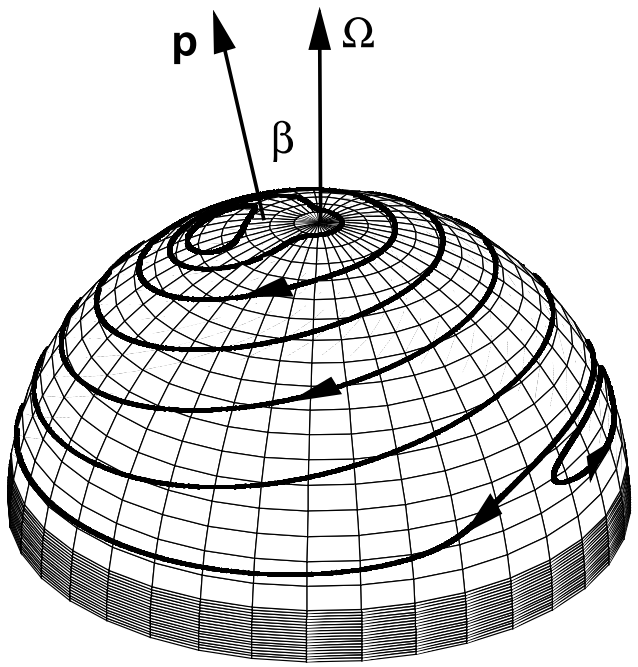


FIG. 3.—Footpoint trajectories on one hemisphere of the source surface in a frame corotating at the equatorial rotation rate of the Sun. The angle between the rotational axis (Ω) and the virtual p-axis (see text for definition) is β. Direction of travel is shown by arrowheads. Note that the trajectory to the far right has a direction of travel that is counterclockwise, opposite to that of the other trajectories. In the shaded region bordering on the solar equator footpoint motion only occurs through diffusive reconnection.

The relationship between the angle β and the tilt angle of the heliospheric current sheet α is given by

$$\beta = \arccos\left[1 - (1 - \cos\theta'_{\rm mm})\left(\frac{\sin^2\alpha}{\sin^2\theta_{\rm mm}}\right)\right] - \alpha, \qquad (5)$$

where $\theta_{\rm mm}$ and $\theta'_{\rm mm}$ are the polar coronal hole boundaries in heliomagnetic coordinates on the photosphere and source surface, respectively (Fisk 1996; Van Niekerk 2000; Krüger 2005). In the original paper of Fisk (1996), it is assumed that the polar coronal hole is symmetric with respect to the magnetic axis. In the current approach, the polar coronal hole on the photosphere is assumed to be symmetric with respect to the rotation axis of the Sun. The quantities $\theta_{\rm mm}$ and $\theta'_{\rm mm}$ should therefore be interpreted as the maximum extend of the polar coronal hole in heliomagnetic coordinates on the photosphere and the source surface, respective. A nominal value for the maximum extend of the polar coronal hole in heliographic coordinates on the photosphere during solar minimum conditions is about 30° (see, e.g., Waldmeier 1981; Bravo & Stewart 1994; Dorotovic 1996; Harvey & Recely 2002). A plausible range for the maximum extend of the polar coronal hole in heliographic coordinates on the source surface during solar minimum conditions is between about 60° and 80° (see, e.g., Munro & Jackson 1977; DeForest et al. 1997; Suess et al. 1998; Cranmer et al. 1999). Here we use a value of 30° for the former (denoted θ_b) and 80° for the latter (denoted θ'_b). It follows that $\theta_{\rm mm} = \theta_b + \alpha$ and $\theta'_{\rm mm} = \theta'_b + \alpha$, and these values are then used when equation (5) is needed in what follows.

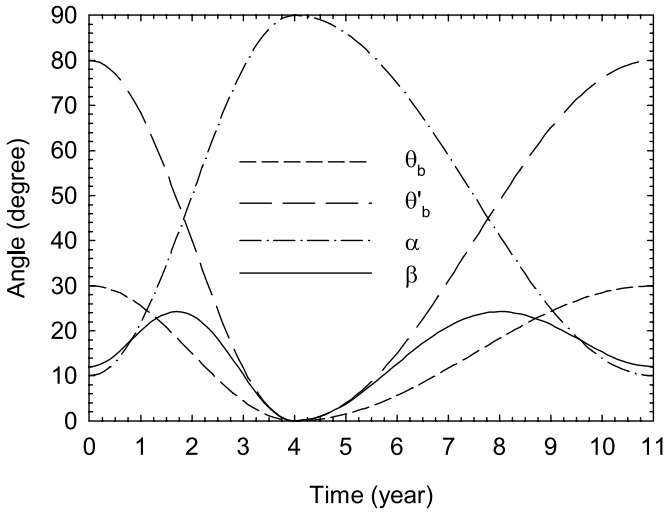


FIG. 4.—Maximum latitudinal extend θ_b of the model polar coronal hole on the photosphere (*short dashed line*) and θ_b' on the source surface (*long dashed line*), the tilt angle of the heliospheric current sheet α (*dot-dashed line*), and the Fisk angle β (*solid line*) as function of time after solar minimum.

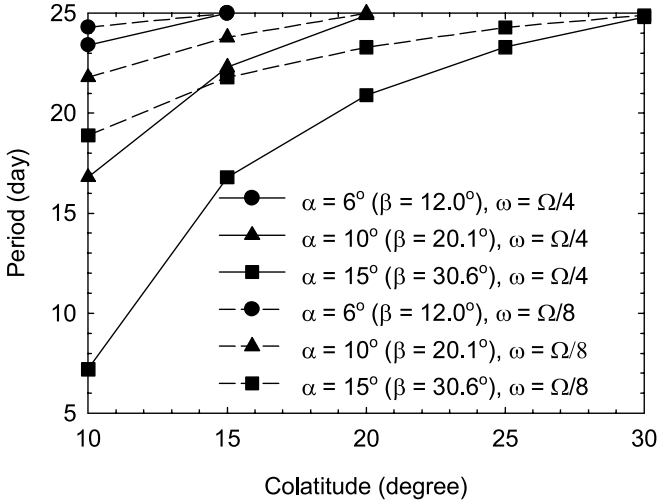


FIG. 5.—Period with which *Ulysses* would observe magnetic feature moving along footpoint trajectories as function of colatitude for various values of the Fisk angle β, denoted by different symbols as indicated in the legend, and for two values of the differential rotation rate ω, $\Omega/4$ (*solid lines*) and $\Omega/8$ (*dashed lines*).

Turning now to the solar cycle dependence of the Fisk-Parker hybrid field, we model the time evolution of the tilt angle of the heliospheric current sheet by

$$\alpha = \alpha_{\min} + \left(\frac{\pi}{4} - \frac{\alpha_{\min}}{2}\right) \times \begin{cases} 1 - \cos\left(\frac{\pi}{4}T\right) & \text{if } 0 \leqslant T \leqslant 4, \\ 1 - \cos\left[\frac{\pi}{7}(T-11)\right] & \text{if } 4 < T \leqslant 11, \end{cases} \quad (6)$$

where the angles are expressed in radians and $\alpha_{\min} = \pi/18$ for the present case. The tilt angle is therefore assumed to vary between 10° and 90°. We further assume that the polar coronal vanishes at solar maximum, and that it has the same time evolution as the tilt angle. This leads to the following expressions for θ_b and θ_b':

$$\theta_b = \frac{\theta_{b,\min}}{2} \begin{cases} 1 + \cos\left(\frac{\pi}{4}T\right) & \text{if } 0 \leqslant T \leqslant 4, \\ 1 + \cos\left[\frac{\pi}{7}(T-11)\right] & \text{if } 4 < T \leqslant 11, \end{cases} \quad (7)$$

$$\theta_b' = \frac{\theta_{b,\min}'}{2} \begin{cases} 1 + \cos\left(\frac{\pi}{4}T\right) & \text{if } 0 \leqslant T \leqslant 4, \\ 1 + \cos\left[\frac{\pi}{7}(T-11)\right] & \text{if } 4 < T \leqslant 11, \end{cases} \quad (8)$$

at a time T years after solar minimum. Here $\theta_{b,\min} = 30^\circ$ and $\theta_{b,\min}' = 80^\circ$ at solar minimum.

Equations (5)–(8) are shown in Figure 4 for an 11 year solar-activity cycle. Note that the Fisk angle β increases from about 12° at solar minimum to 24° before becoming zero at solar maximum.

Our current model for the time evolution of the heliospheric tilt angle (eq. [6]) is obviously an oversimplification, and is used here to give a qualitative idea of how the Fisk-type field could evolve over the course of a solar cycle. In any attempt to study cosmic-ray modulation over 11 or 22 yr, changes in the magnitude of the solar magnetic field and all the other quantities shown in § 4 also have to be taken into account.

3. OBSERVATIONAL CONSTRAINTS ON THE HYBRID FIELD

The question of whether a Fisk-type field actually exists has—as was pointed out in the introduction—received some attention. The obvious starting point is to look for its signature in magnetic field data. This has been done, but with conflicting results (see, e.g., Zurbuchen et al. 1997; Forsyth et al. 2002; Roberts et al. 2007). Equation (4) predicts that a fixed observer should see a periodicity in magnetic field data at the solar equatorial rotation rate. Zurbuchen et al. (1997) point out a second periodicity. This occurs when the transit time of a magnetic feature along a footpoint trajectory matches the transit time of the spacecraft in its orbit between two points of intersection; this is described in detail by Zurbuchen et al. (1997) and also by Van Niekerk (2000). Van Niekerk considered other colatitudes than the 20° of Zurbuchen et al. (1997) but for a constant differential rotation rate. Here we also consider changes in the latter for a pure Fisk field using the same basic parameters as Zurbuchen et al. (1997) shown in Figure 5. For $\beta \approx 30^\circ$ (*filled squares*) and $\omega = \Omega/4$ (*solid line*), the values used by Zurbuchen et al. (1997) the observed period can vary from about 7 days at 10° colatitude to the solar equatorial period of 25 days at 30° colatitude. The period increases if either β or ω is decreased, and for $\beta = 12^\circ$ and $\omega \leqslant \Omega/4$ it would be barely distinguishable from the solar equatorial period even at the highest latitudes. Note that the latter values are those used in the current paper for solar minimum conditions. The next question is whether the amplitude of the fluctuations in the field is at a high enough level to be observable above the random turbulent level. The answer is provided by Roberts et al. (2007), who show that a value of β that is smaller than about 15° would be consistent with observations, but hard to be distinguished from noise. We therefore conclude that a hybrid field with $\beta = 12^\circ$ should not be observable in magnetic field data.

The analysis of Roberts et al. (2007) shows a very significant period of around 27 days in the solar wind velocity, especially in the radial component. Given the fact that the Parker model of the heliospheric magnetic field has an azimuthal component that is inversely proportional to the solar wind speed, one would then expect to see a similar significant periodicity in this component of the magnetic field, but their analysis shows that this is

certainly not always observed. The question now becomes, if the period that one would expect to see in the well-established Parker field's azimuthal component is not observed, should one expect to see the predicted periods of the Fisk-type field? It could be that the periods we expect to see in either field is masked by temporal changes in the field, or that the period in the solar wind speed is not always seen in the field components because footpoint motion is masking it, i.e., the field is really a Fisk-type field.

4. MODULATION MODEL

The current modulation study is limited to solar minimum conditions. Krüger (2005) did consider periods of increased solar activity, but used a different diffusion tensor.

We use a steady state, three-dimensional modulation model (Kóta & Jokipii 1983; Burger & Hattingh 1995; Hattingh & Burger 1995; Hattingh 1998) to solve Parker's transport equation (Parker 1965) for the cosmic-ray distribution function at position $\boldsymbol{r}$ and with momentum p,

$$\nabla \cdot \left(\mathbf{K}^S \cdot \nabla f\right) - (\boldsymbol{v}_d + \boldsymbol{V}_{\rm sw}) \cdot \nabla f + \frac{1}{3}(\nabla \cdot \boldsymbol{V}_{\rm sw}) \frac{\partial f}{\partial \ln p} = \frac{\partial f}{\partial t}, \quad (9)$$

where $\boldsymbol{v}_d = \nabla \times (\kappa_{\rm A} \boldsymbol{B}/B_0)$ (see eq. [16] below) is the drift velocity, where $\boldsymbol{B}$ is the steady state version of the heliospheric magnetic field (eq. [4]) and B_0 is its magnitude, $\boldsymbol{V}_{\rm sw}$ is the solar wind velocity, and $\mathbf{K}^S$ is the symmetric part of the diffusion tensor,

$$\mathbf{K} = \begin{bmatrix} \kappa_\parallel & 0 & 0 \\ 0 & \kappa_{\perp,2} & \kappa_{\rm A} \\ 0 & -\kappa_{\rm A} & \kappa_{\perp,3} \end{bmatrix}. \quad (10)$$

The distribution function $f(\boldsymbol{r}, p)$ is related to the differential intensity with respect to kinetic energy, j_T, by $j_T = p^2 f$.

The tilt angle of the heliospheric current sheet is 10° (see eq. [6]), the solar wind speed $V_{\rm sw} = 600$ km s^{-1}, and the outer boundary is at 50 AU. The latter value is chosen due to computing restrictions. Equation (9) is solved over the whole of this model heliosphere.

The parallel diffusion coefficient, adapted from the random sweeping model for dynamical slab turbulence of Teufel & Schlickeiser (2003) is given by

$$\kappa_\parallel = \frac{B_0^2}{\delta B_{\rm slab}^2} \frac{3\nu_I}{\sqrt{\pi}(\nu_I - 1)} \frac{k_{\rm min} R_L^2}{b} \times \left\{ \frac{b}{4\sqrt{\pi}} + \frac{2}{\sqrt{\pi}(2-\nu_I)(4-\nu_I)} \frac{b}{R^{\nu_I}} + \left[\frac{1}{\Gamma(\nu_D/2)} + \frac{1}{\sqrt{\pi}(\nu_D - 2)} \right] \frac{b^{\nu_D - 1}}{R^{\nu_I} Q^{\nu_D - \nu_I}} \right\}, \quad (11)$$

where B_0 is the magnitude of the background heliospheric magnetic field, $\delta B_{\rm slab}^2$ is the variance of the slab component of the turbulence, ν_I and ν_D are the spectral indices in the inertial and dissipation ranges, respectively, Γ is the gamma function, $R_L = P/B_0$ is the (maximal) Larmor radius with $P = pc/|q|$ particle rigidity, $k_{\rm min}$ is the wavenumber associated with the transition from the energy to the inertial range of the slab power spectrum, and

$$R = k_{\rm min} R_L, \quad (12)$$

$$b = \frac{v}{2\alpha_d v_{\rm A}}, \quad (13)$$

$$Q = k_D R_L, \quad (14)$$

where v is particle speed, α_d is a parameter which determines the strength of dynamical effects (Bieber et al. 1994; Teufel & Schlickeiser 2002), $v_{\rm A}$ is the Alfvèn speed, and k_D is the wavenumber associated with the transition from the inertial to the dissipation range of the slab power spectrum. We choose this particular representation for the parallel diffusion coefficient because it gives an analytical expression which can be used to study the transport of low-energy electrons. Commenting on the usefulness of quasi-linear theory, Minnie et al. (2007a) report good agreement with the simulated mean free paths from their direct numerical simulations of charged-particle transport in a turbulent magnetic field for low levels of turbulence.

For diffusion perpendicular to the background field we use the nonlinear guiding center (NLGC) theory of Matthaeus et al. (2003). Shalchi et al. (2004) provide analytical approximations for the results from this theory (see also Zank et al. 2004), and we use

$$\kappa_\perp = \left[a^2 v \frac{\nu_I - 1}{2\sqrt{3}\nu_I} \sqrt{\pi} \frac{\Gamma(\nu_I/2 + 1)}{\Gamma(\nu_I/2 + 1/2)} l_{\rm 2D} \frac{\delta B_{\rm 2D}^2}{B_0^2} \right]^{2/3} \kappa_\parallel^{1/3}, \quad (15)$$

where a is a constant and $\delta B_{\rm 2D}^2$ and $l_{\rm 2D}$ are the variance and the correlation length of the 2D component of the turbulence, respectively. Other quantities are defined in equation (11). To calculate $\kappa_\perp$ in equation (15), we use $\kappa_\parallel$ from equation (11).

The fact that drift is reduced by the presence of turbulence has been established by direct numerical simulations (see, e.g., Giacalone et al. 1999; Minnie et al. 2007b, and references therein). The functional form for the reduction has, however, not been unambiguously established, and we choose a simple one that depends only on particle rigidity,

$$\kappa_{\rm A} = \frac{pv}{3qB_0} \frac{(P/P_0)^2}{1 + (P/P_0)^2}, \quad (16)$$

where $P_0 = 1/\sqrt{2}$ GV. For the turbulence quantities we use simple approximations, and assume that

$$k_{\rm min} = 32 r^{0.5} \ {\rm AU}^{-1},$$
$$k_D = 3 \times 10^6 (B_0/B_{\rm Earth}) \ {\rm AU}^{-1},$$
$$l_{\rm 2D} = \left(3.1 \times 10^{-3}\right) r^{-0.5} \ {\rm AU},$$
$$\delta B_{\rm slab}^2 = 0.2\left(25 r^{-2.5}\right) \ {\rm nT}^2,$$
$$\delta B_{\rm 2D}^2 = 0.8\left(25 r^{-2.5}\right) \ {\rm nT}^2.$$

Note that we use a composite model for the turbulence, with 20% slab and 80% 2D turbulence (see, e.g., Bieber et al. 1996). Other relevant parameters are solar wind density = 7 protons cm^{-3}, $a = 1/\sqrt{3}$, $\nu_I = 5/3$, $\nu_D = 2.6$, $B_{\rm Earth} = 4.2$ nT, and $\alpha_d = 1$. For the present study we assume isotropic perpendicular diffusion, with $\kappa_{\perp,2} = \kappa_{\perp,3} = \kappa_\perp$.

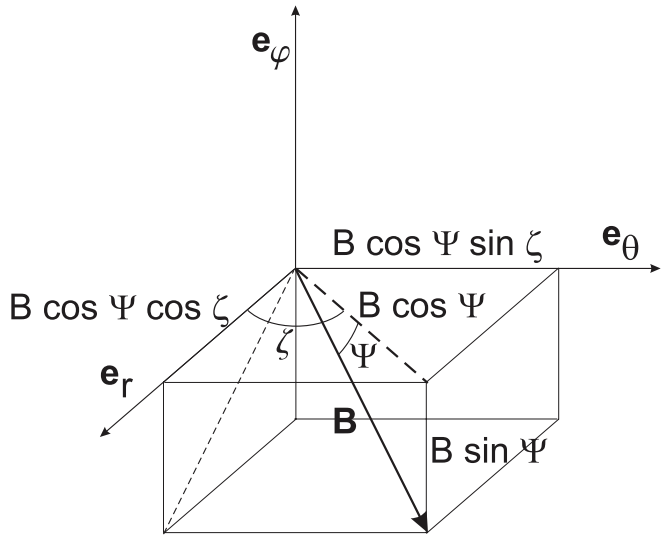


FIG. 6.—Coordinate system showing the angles Ψ and ζ used in the transformation from field-aligned to spherical coordinates, resulting in the elements given in expression (17).

For completeness, we note that a transformation from field-aligned to spherical coordinates yields a tensor with elements

$$\begin{aligned}
\kappa_{rr} &= \kappa_{\perp,2}\sin^2\zeta + \cos^2\zeta\left(\kappa_{||}\cos^2\Psi + \kappa_{\perp,3}\sin^2\Psi\right),\\
\kappa_{r\theta} &= -\kappa_{\rm A}\sin\Psi + \sin\zeta\cos\zeta\\
&\quad\times\left(\kappa_{||}\cos^2\Psi + \kappa_{\perp,3}\sin^2\Psi - \kappa_{\perp,2}\right),\\
\kappa_{r\phi} &= -\kappa_{\rm A}\cos\Psi\sin\zeta - \left(\kappa_{||} - \kappa_{\perp,3}\right)\sin\Psi\cos\Psi\cos\zeta,\\
\kappa_{\theta r} &= \kappa_{\rm A}\sin\Psi + \sin\zeta\cos\zeta\\
&\quad\times\left(\kappa_{||}\cos^2\Psi + \kappa_{\perp,3}\sin^2\Psi - \kappa_{\perp,2}\right),\\
\kappa_{\theta\theta} &= \kappa_{\perp,2}\cos^2\zeta + \sin^2\zeta\left(\kappa_{||}\cos^2\Psi + \kappa_{\perp,3}\sin^2\Psi\right),\\
\kappa_{\theta\phi} &= \kappa_{\rm A}\cos\Psi\cos\zeta - \left(\kappa_{||} - \kappa_{\perp,3}\right)\sin\Psi\cos\Psi\sin\zeta,\\
\kappa_{\phi r} &= \kappa_{\rm A}\cos\Psi\sin\zeta - \left(\kappa_{||} - \kappa_{\perp,3}\right)\sin\Psi\cos\Psi\cos\zeta,\\
\kappa_{\phi\theta} &= -\kappa_{\rm A}\cos\Psi\cos\zeta - \left(\kappa_{||} - \kappa_{\perp,3}\right)\sin\Psi\cos\Psi\sin\zeta,\\
\kappa_{\phi\phi} &= \kappa_{||}\sin^2\Psi + \kappa_{\perp,3}\cos^2\Psi, \qquad (17)
\end{aligned}$$

where $\tan\Psi = -B_\phi/\left(B_r^2 + B_\theta^2\right)^{1/2}$ and $\tan\zeta = B_\theta/B_r$. Note that Alania & Dzhapiashvili (1979), Alania (2002), and Kobylinski (2001) give a similar result, but with $\tan\Psi = -B_\phi/B_r$. The relevant angles are shown in Figure 6. Finally, the respective local interstellar spectra for helium, protons, and electrons are given in the Appendix.

5. SAMPLE SOLUTIONS

In § 3 we have argued that the Fisk-Parker hybrid field, with parameters appropriate for solar minimum conditions as given in § 2, would not be observable in magnetic field data. Here we show that the signature of a Fisk-type should, however, be clearly visible in particle data. Our aim with this paper is to concentrate on qualitative behavior rather than to try and fit any particle data set.

In what follows, we use global latitude gradients, defined for a given rigidity as

$$G_\theta(r) = \frac{\ln\left[\langle j_T(r,\theta_2,\phi)\rangle_\phi / \langle j_T(r,\theta_1,\phi)\rangle_\phi\right]}{\Delta\theta}\times 100\%, \qquad (18)$$

where $j_T(r,\theta)$ is the differential intensity at a heliocentric distance r and colatitude θ, and $\Delta\theta = \theta_1 - \theta_2$. We always use co-

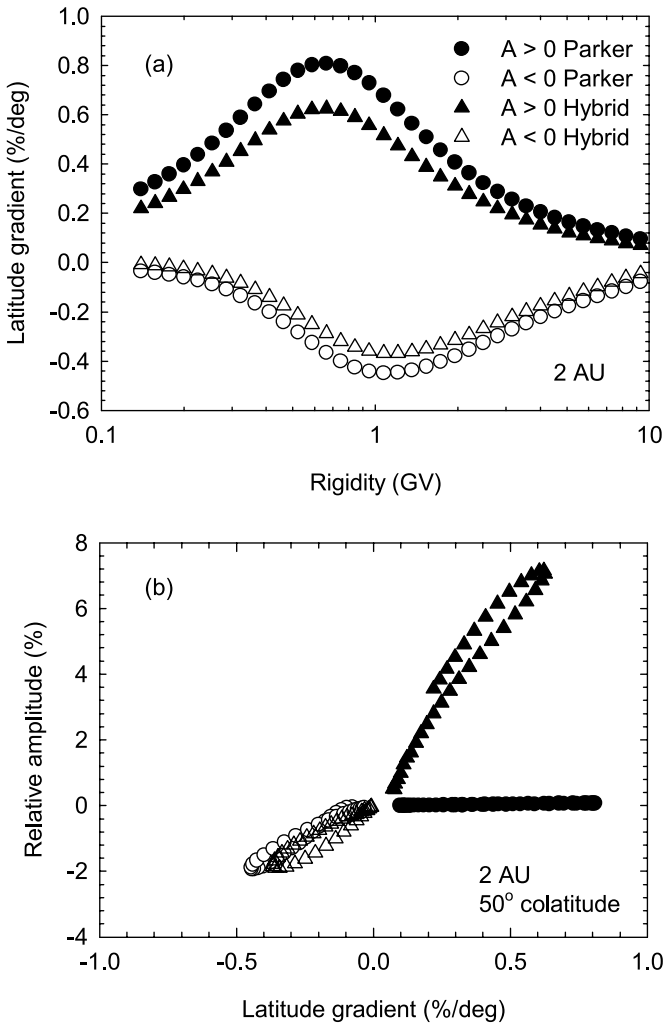


FIG. 7.—(*a*) Global latitude gradient as function of rigidity, and (*b*) amplitude of 26 day proton variations at colatitude 50° as function of global latitude gradient, both at a radial distance of 2 AU, for the Fisk-Parker hybrid field (*triangles*) and a standard Parker field (*circles*). Filled symbols denote $qA > 0$ solar magnetic polarity, and open symbols $qA < 0$ solar magnetic polarity.

latitudes $\theta_2 = 10^\circ$ and $\theta_1 = 90^\circ$, and either $r = 1$ or 2 AU. Following Zhang (1997), we define the amplitude of the recurrent cosmic-ray variations at a given rigidity as

$$\Delta j_T(r,\theta) = \frac{j_T^{\max}(r,\theta,\phi) - j_T^{\min}(r,\theta,\phi)}{\langle j_T(r,\theta,\phi)\rangle_\phi}\times 100\%, \qquad (19)$$

and make it negative if the associated latitude gradient is negative.

Figure 7*a* shows that a Fisk-Parker hybrid field (*triangles*) produces smaller latitude gradients than a Parker field (*circles*), confirming the results of Burger & Hitge (2004), who used a different diffusion tensor. Note that solutions for a Parker field are obtained by setting $F_S = 0$ in equation (4) for the hybrid field. The relative amplitude of the cosmic-ray variations as function of latitude gradient at a colatitude of 50° for the Fisk-type field (*triangles*) in Figure 7*b* shows a number of interesting features. First, it explains the scatter in the simulated data of the similar figure in Burger & Hitge (2004), who only used a limited number of points: the relationship between the two quantities is not a single straight line; the behavior is slightly different for high and for low rigidities, resulting in loops rather than straight lines. To put this another way, if the latitude gradient is the same for

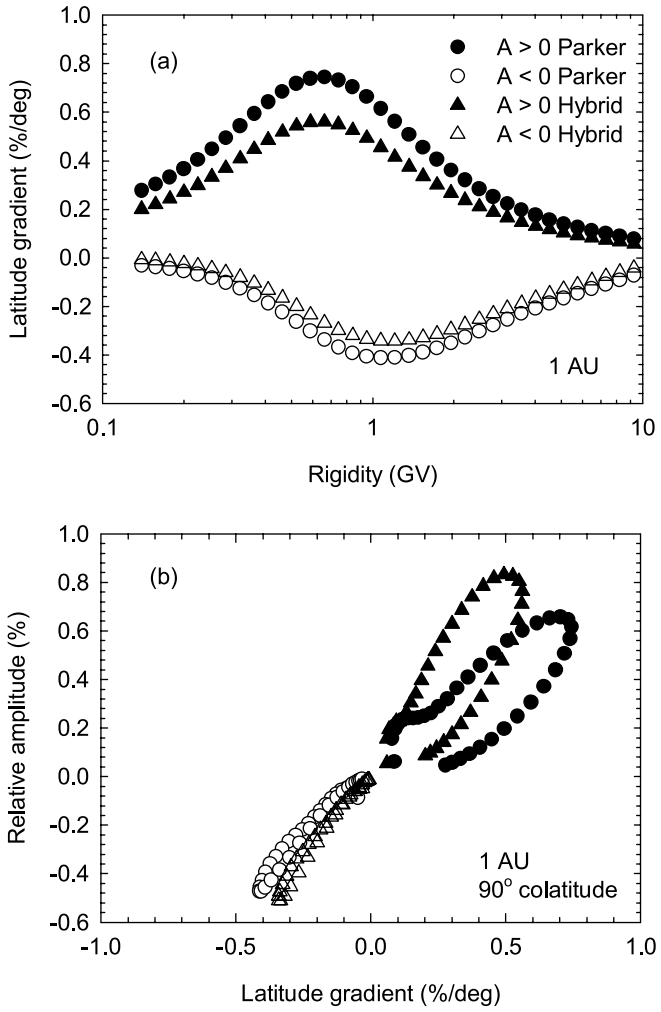


FIG. 8.—Same as Fig. 7, but with (*a*) for 1 AU, and (*b*) for a colatitude of 90° and also 1 AU.

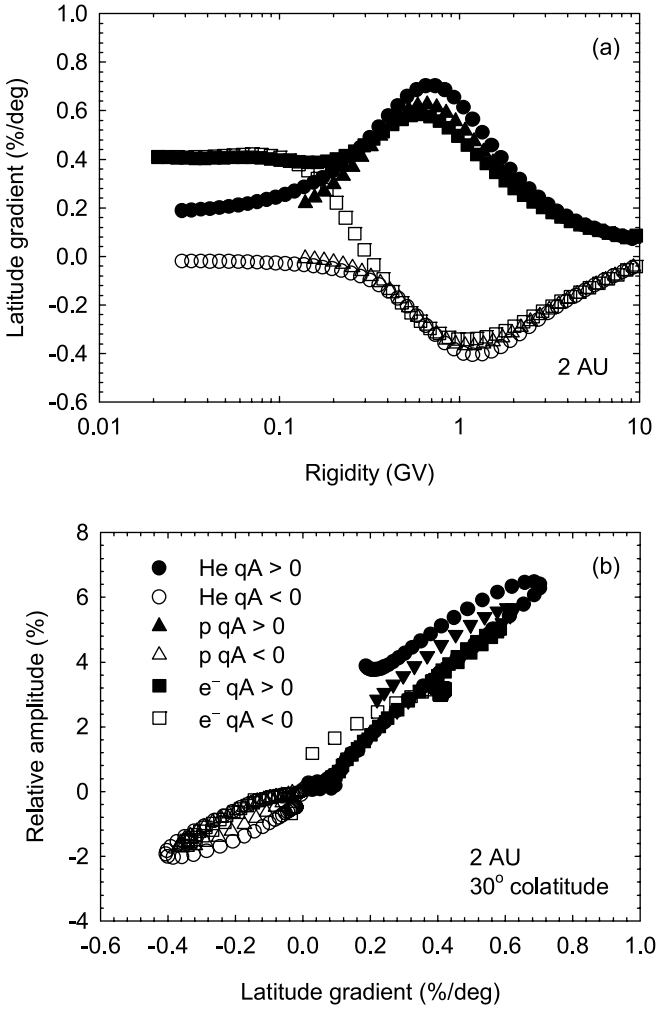


FIG. 9.—(*a*) Global latitude gradient as function of rigidity, and (*b*) amplitude of 26 day proton variations at colatitude 30° as function of global latitude gradient, both at a radial distance of 2 AU, for the Fisk-Parker hybrid field. Helium is denoted by circles, protons by triangles, and electrons by squares. Filled symbols denote $qA > 0$ solar magnetic polarity, and open symbols $qA < 0$ solar magnetic polarity.

particles with different rigidities, the relative amplitudes of the cosmic-ray variations are not necessarily identical. The second feature is that the constant of proportionality is different for the two solar magnetic field polarities. This feature was inferred from near-Earth particle data by Richardson et al. (1999). A third prominent feature is seen when the variations for a Fisk-type field (*triangles*) are compared with the variations for a Parker field (*circles*). For $A > 0$ (*filled symbols*), when particles are drifting from the solar polar regions of the heliosphere to the equatorial region, there are no recurrent variations in the simulated particle data for a Parker field at this colatitude. For $A < 0$ (*open symbols*), when the drift direction is changed, recurrent variations are present for both fields. This property of the Parker field is expected, and is due to the interaction of particles with the wavy current sheet. For this magnetic polarity cycle the signature of the interaction is present far beyond latitudes where the wavy current sheet is present (see e.g., Fig. 1 of Kóta & Jokipii 1983).

Figure 8 is similar to Figure 7, but is for a radial distance of 1 AU, and for recurrent variations in the equatorial plane, a colatitude of 90°. While the latitude gradients are very similar to those at 2 AU, there are important differences in the recurrent variations. Most notable is that recurrent variations for the Parker field are present for both solar magnetic cycles, obviously caused by the wavy current sheet. The Fisk-type field gives slightly larger amplitudes than the Parker field for the same latitude gradients when $A < 0$; the difference is in the same direction but more pronounced when $A > 0$. While the difference in the constant of proportionality for the Fisk-type field for the two magnetic cycles is much less noticeable than at high latitudes, the constant of proportionality for the Parker field when $A > 0$ is clearly smaller than when $A < 0$. Overall, the Fisk-type fields gives larger recurrent variations when $A > 0$ than when $A < 0$; surprisingly, the same is seen for the Parker field, although not as pronounced. We know from accompanying runs that the shape of these curves is sensitive to the choice of diffusion tensor especially in the equatorial region and at this time we refrain from making general conclusions.

In Figure 9 we show latitude gradients and the amplitude of recurrent variations for three different species, helium, protons, and electrons, for both solar magnetic field polarities. The latitude gradients of the three species in Figure 9*a* are very similar for rigidities above about 0.5 GV. Below this value, those for helium and protons are still similar, but the latitude gradient for electrons for $qA < 0$ decreases, changes sign, and increases again. Below about 0.2 GV, the latitude gradients for the two magnetic cycles are the same. The amplitude of recurrent variations for three different species in Figure 9*b* are qualitatively

similar for all latitude gradients, and almost identical for those latitude gradients associated with high rigidities. In fact, for $qA > 0$, the constants of proportionality for best fits (not shown) differ by less than 10% between the three species. The width of the loops are the largest for helium and the smallest for electrons. Taken together, the three data sets also show different constants of propotionality for the two solar magnetic cycles. The difference is, however, less pronounced than that at the higher colatitude (i.e., lower latitude) in Figure 7*b*.

Note that the almost linear relationship between the amplitude of the recurrent cosmic-ray variations and the global latitude gradient for the Fisk-Parker hybrid field is in qualitative agreement with the observational results of Zhang (1997) and Paizis et al. (1999).

6. SUMMARY AND CONCLUSIONS

In this paper we present a refinement of the Fisk-Parker hybrid field of Burger & Hitge (2004), which now includes a region bordering the solar rotational equator where magnetic field footpoint motion occurs only through diffusive reconnection. At high latitudes the field is a mixture of Fisk field and Parker field, and in the equatorial region it is a pure Parker field. We also propose a simple model for the solar cycle dependence of the hybrid field, taking into account changes in the tilt angle of the heliospheric current sheet and the latitudinal extend of the polar coronal hole on the photosphere and on the source surface over the course of a solar activity cycle. Using the results of Roberts et al. (2007), we deduce that the amplitude of magnetic field fluctuations for assumed solar minimum parameters would not be observable about the background noise. We also show that for these parameters, periodicities associated with differential footpoint motion would be barely distinguishable from the solar equatorial period.

We confirm the result of Burger & Hitge (2004) that a Fisk-type heliospheric magnetic field provides a natural explanation for the observed linear relationship between the amplitude of the recurrent cosmic-ray variations and the global latitude gradient, first reported by Zhang (1997). We show that this relationship holds for helium, protons, and electrons. Moreover, we show that the constant of proportionality is larger when $qA > 0$ than when $qA < 0$, as inferred from observations by Richardson et al. (1999).

It is also clear that the question of periodicities in magnetic field data is perhaps more complicated than previously thought. We point out that given the strong periodicity in the solar wind speed observed by Roberts et al. (2007) the lack of an ubiquitous strong periodicity in the azimuthal component of the magnetic field may be explained by the existence of a Fisk-type field.

Our model for a Fisk-type field was constructed to be as simple as possible. It clearly does not include all the complicated azimuthal dependent structures that such a field should have, nor is it time dependent. The question should not be if this field is fully realistic, but rather if it did exist, would it be observable in magnetic field data and could it explain at least some particle measurements that as yet have no other generally accepted explanation. We believe that the answers to these two questions are no and yes, respectively.

R. A. B. thanks Len Fisk and Randy Jokipii for helpful discussions. This material is based on work supported by the National Research Foundation and NASA grant NNX07AH73G.

APPENDIX

LOCAL INTERSTELLAR SPECTRA

The local interstellar spectrum (LIS) for protons is identical to that of Bieber et al. (1999) at high energy but higher at low energy. It is expressed in terms of particle rigidity as

$$j^{p}_{\rm LIS} = 19.0\frac{(P/P_0)^{-2.78}}{1+(P_0/P)^2}, \tag{A1}$$

in units of particles $\rm m^{-2}\ s^{-1}\ sr^{-1}\ MeV^{-1}$ with $P_0 = 1$ GV and P in GV. This spectrum is similar to that of Caballero-Lopez et al. (2004), but slightly higher at lower rigidities. For helium we use

$$j^{\rm He}_{\rm LIS} = 5.0\frac{(P/P_0)^{-2.7}}{\left[1+(P_0/P)^2\right]^{1.25}}, \tag{A2}$$

where the symbols and units are the same as for equation (A1). This spectrum is again similar to that of Caballero-Lopez et al. (2004). The electron LIS is from Langner et al. (2001) parameterized by Langner (2004) as

$$j^{\rm elec}_{\rm LIS} = \begin{cases} \dfrac{214.32+3.32\ln(P/P_0)}{1+0.26\ln(P/P_0)+0.02[\ln(P/P_0)]^2} & \text{if } P < 0.0026 \text{ GV}, \\ 1.7\left[\dfrac{52.55+23.01(P/P_0)}{1+148.62(P/P_0)}\right]^2 & \text{if } 0.0026 \text{ GV} \le P < 0.1 \text{ GV}, \\ \dfrac{1555.89+17.36(P/P_0)-3.4\times10^{-3}(P/P_0)^2+5.13\times10^{-7}(P/P_0)^3}{1-11.22(P/P_0)+7532.93(P/P_0)^2+2405.01(P/P_0)^3+103.87(P/P_0)^4} & \text{if } 0.1 \text{ GV} \le P \le 10.0 \text{ GV}, \\ 1.7\exp[-0.89-3.22\ln(P/P_0)] & \text{if } P > 10 \text{ GV}, \end{cases} \tag{A3}$$

in units of particles $\rm m^{-2}\ s^{-1}\ sr^{-1}\ MeV^{-1}$ with $P_0 = 1$ GV and P in GV.

REFERENCES

Alania, M. V. 2002, Acta Phys. Polonia B, 33, 1149
Alania, M. V., & Dzhapiashvili, T. V. 1979, in Proc. 16th Int. Cosmic Ray Conf. (Tokyo), 19
Bieber, J. W., Burger, R. A., Engel, R., Gaisser, T. K., Roesler, S., & Stanev, T. 1999, Phys. Rev. Lett., 83, 674
Bieber, J. W., Matthaeus, W. H., Smith, C. W., Wanner, W., Kallenrode, M.-B., & Wibberenz, G. 1994, ApJ, 420, 294
Bieber, J. W., Wanner, W., & Matthaeus, W. H. 1996, J. Geophys. Res., 101, 2511
Bravo, S., & Stewart, G. 1994, Sol. Phys., 154, 377
Burger, R. A. 2005, Adv. Space Res., 35, 636
Burger, R. A., & de Jager, O. C. 2003, in AGU 2003 Fall Meeting, SH11C-28
Burger, R. A., & Hattingh, M. 1995, Ap&SS, 230, 375
Burger, R. A., & Hitge, M. 2002, in AGU 2002 Fall Meeting, SH71A-04
———. 2004, ApJ, 617, L73
Burger, R. A., van Niekerk, Y., & Potgieter, M. S. 2001, Space Sci. Rev., 97, 331
Caballero-Lopez, R. A., Moraal, H., McCracken, K. G., & McDonald, F. B. 2004, J. Geophys. Res., 109, A12102
Cranmer, S. R., et al. 1999, ApJ, 511, 481
DeForest, C. E., Hoeksema, J. T., Gurman, J. B., Thompson, B. J., Plunkett, S. P., Howard, R., Harrison, R. C., & Hasslerz, D. M. 1997, Sol. Phys., 175, 393
Dorotovic, I. 1996, Sol. Phys., 167, 419
Fisk, L. A. 1996, J. Geophys. Res., 101, 15547
———. 2001, J. Geophys. Res., 106, 15849
———. 2005, ApJ, 626, 563
Fisk, L. A., & Schwadron, N. A. 2001, ApJ, 560, 425
Fisk, L. A., & Zurbuchen, T. H. 2006, J. Geophys. Res., 111, A09115
Forsyth, R. J., Balogh, A., & Smith, E. J. 2002, J. Geophys. Res. Space Phys., 107, 1405
Fox, P., McIntosh, P., & Wilson, P. R. 1998, Sol. Phys., 177, 375
Giacalone, J. 1999, Adv. Space Res., 23, 581
———. 2001, J. Geophys. Res., 106, 15881
Giacalone, J., Jokipii, J. R., & Kóta, J. 1999, in Proc. 26th Int. Cosmic Ray Conf. (Salt Lake City), 37
Giacalone, J., Jokipii, J. R., & Matthaeus, W. H. 2006, ApJ, 641, L61
Harvey, K. L., & Recely, F. 2002, Sol. Phys., 211, 31
Hattingh, M. 1998, Ph.D. thesis, Potchefstroomse Univ.
Hattingh, M., & Burger, R. A. 1995, Adv. Space Res., 16, 213
Kobylinski, Z. 2001, Adv. Space Res., 27, 541
Kóta, J., & Jokipii, J. R. 1983, ApJ, 265, 573
———. 1997, in Proc. 25th Int. Cosmic Ray Conf., Vol. 2 (Durban), 25
———. 1999, in Proc. 26th Int. Cosmic Ray Conf., Vol. 7 (Salt Lake City), 9
———. 2001, in AGU Fall Meeting, SH22A-51
Krüger, T. P. J. 2005, M.S. thesis, North-West Univ. (Potchefstroom Campus)
Langner, U. W. 2004, Ph.D. thesis, Potchefstroomse Univ.
Langner, U. W., de Jager, O. C., & Potgieter, M. S. 2001, Adv. Space Res., 27, 517
Lionello, R., Linker, J. A., Mikić, Z., & Riley, P. 2006, ApJ, 642, L69
Matthaeus, W. H., Qin, G., Bieber, J. W., & Zank, G. P. 2003, ApJ, 590, L53
Minnie, J., Bieber, J. W., Matthaeus, W. H., & Burger, R. A. 2007a, ApJ, 663, 1049
———. 2007b, ApJ, 670, 1149
Munro, R. H., & Jackson, B. V. 1977, ApJ, 213, 874
Paizis, C., et al. 1999, J. Geophys. Res., 104, 28241
Parker, E. N. 1958, ApJ, 128, 664
———. 1965, Planet. Space Sci., 13, 9
Pei, C., Jokipii, J. R., & Giacalone, J. 2006, ApJ, 641, 1222
Richardson, I. G., Cane, H. V., & Wibberenz, G. 1999, J. Geophys. Res., 104, 12549
Roberts, D. A., Giacalone, J., Jokipii, J. R., Goldstein, M. L., & Zepp, T. D. 2007, J. Geophys. Res., 112, A08103
Roberts, D. A., & Goldstein, M. L. 1998, Geophys. Res. Lett., 25, 595
Schou, J., et al. 1998, ApJ, 505, 390
Schwadron, N. A. 2002, Geophys. Res. Lett., 29, 8
Shalchi, A., Bieber, J. W., & Matthaeus, W. H. 2004, ApJ, 604, 675
Simpson, J. A., Zhang, M., & Bame, S. 1996, ApJ, 465, L69
Simpson, J. A., et al. 1995, Science, 268, 1019
Suess, S. T., Poletto, G., Wang, A.-H., Wu, S. T., & Cuseri, I. 1998, Sol. Phys., 180, 231
Teufel, A., & Schlickeiser, R. 2002, A&A, 393, 703
———. 2003, A&A, 397, 15
Van Niekerk, Y. 2000, M.S. thesis, Potchefstroomse Univ.
Waldmeier, M. 1981, Sol. Phys., 70, 251
Woo, R., Habbal, S. R., Howard, R. A., & Korendyke, C. M. 1999, ApJ, 513, 961
Zank, G. P., Gang, L., Florinski, V., Matthaeus, W. H., Webb, G. M., & le Roux, J. A. 2004, J. Geophys. Res., 109, A04107
Zhang, M. 1997, ApJ, 488, 841
Zurbuchen, T. H., Schwadron, N. A., & Fisk, L. A. 1997, J. Geophys. Res., 102, 24175